Control mechanism of friction by dynamic actuation of nanometer-sized contacts

Hiroyuki Iizuka, Jun Nakamura,* and Akiko Natori†
Department of Electronic-Engineering, The University of Electro-Communications (UEC-Tokyo), 1-5-1 Chofugaoka, Chofu, Tokyo 182-8585, Japan

(Received 24 April 2009; revised manuscript received 16 July 2009; published 26 October 2009)

We studied both the mechanism and the condition of dynamic superlubricity actuated in a dynamic way for the atomic contact of a friction force microscope, using dynamical simulation of the Tomlinson model. The superlubricity was achieved by ac modulation of the normal force acting between two contacting bodies at well-defined frequencies corresponding to normal resonances of the combined system [A. Socoliuc *et al.*, Science **313**, 207 (2006)]. The time-averaged friction force depends crucially on the modulation amplitude and the superlubricity occurs above the critical amplitude. The effect on the superlubricity of the corrugation amplitude of surface potential, sliding velocity, a damping coefficient, and temperature are clarified. The superlubricity at zero temperature can be induced by transit of the tip via the "turning point," the top position of the surface potential without elastic deformation, and it is allowed at low-sliding velocities in the underdamped case. The superlubricity at a room temperature can be actuated efficiently with a much smaller critical amplitude than that at zero temperature and it can be achieved at sufficiently low-sliding velocities in both the underdamped and the overdamped cases, assisted by thermally activated hopping of the tip.

DOI: 10.1103/PhysRevB.80.155449 PACS number(s): 68.35.Af, 07.79.Sp, 81.40.Pq, 46.55.+d

I. INTRODUCTION

Scientists and engineers have long been intrigued by the phenomena of friction and a friction force microscope (FFM) was developed as a new ideal experimental method to detect friction on the atomic scale. Mate *et al.* reported the first observation of a stick-slip movement of the tip with atomic periodicity of the sample surface structure.[1] The energy is dissipated at the abrupt slip and, hence, the stick-slip motion is the origin of friction on the atomic scale. The stick-slip motion is suppressed and continuous sliding occurs without energy dissipation, when the corrugation amplitude of the surface potential is decreased below a critical threshold.

Several ways to reduce friction have been proposed and sliding with negligible friction is called as superlubricity.[2] When two surfaces in contact are laterally stiff and incommensurate, superlubricity appears since the effective corrugation of the surface potential can be reduced less than the threshold. Indeed, Dienwiebel *et al.* have observed superlubricity while turning a graphite flake out of registry over a graphite surface.[3] Recently, we also demonstrated superlubricity at the magic size for multiatomic contacts with surface in the lattice-mismatched case.[4] The corrugation amplitude of surface potential can also be reduced by decreasing normal load acting on the tip.[5] On the other hand, friction at a finite temperature can be reduced as the sliding speed is decreased.[6,7] Thermally activated jumps of the tip are enhanced at low-sliding velocity and this superlubricity is called as thermolubricity.

Recently, atomic scale control of friction has also been tried by actuation of nanometer-sized contacts. Riedo *et al.* tried torsional oscillation of the cantilever.[8] The average friction force was found to be resonantly reduced by superimposing torsional oscillation on a cantilever at low-scan velocity, while no resonant reduction was observed at high-scan velocity. They ascribed the observed resonant reduction to activation of oscillation of the tip at the stick point. Socoliuc *et al.*, on the other hand, succeeded in achieving superlubricity in a dynamic way by exciting the mechanical resonances of the sliding system perpendicular to the contact plane.[9] They attributed the resonant reduction to the induced dynamical modulation of corrugation amplitude of the surface potential and predicted the critical amplitude using the adiabatic approximation. Very recently, the dynamic superlubricity offered a way to avoid the wear of tiny silicon tips in the "write-read" action of data storage.[10]

A number of experimental results obtained by a friction force microscope have been explained successfully by a Tomlinson model,[11] in which single spring and an atomic-scale tip are assumed. The cantilever and the contact of FFM are thought to act as springs in series and this picture gives the single spring model with the effective spring constant. The appearance condition of stick-slip as a function of load[5,8] and the occurrence of slip over multiple lattice units[1,12–16] have been analyzed satisfactorily. Furthermore, dependence of the atomic friction on the scanning velocity, V, has also been elucidated by including thermal activation of the slip motion.[7,15,17] Recently, a nonmonotonic dependence of friction on temperature has been observed in FFM measurement[18] and it has been explained by competition between two factors, thermal activation of the slip motion and decrease in the slip length with temperature.[19] As for the resonant reduction by torsional oscillation,[8] a remarkable reduction of the average friction force was shown to occur at two characteristic oscillation frequencies, with use of computer simulation in the Tomlinson model.[20] The first frequency is an oscillation frequency of the tip atom at the stick point, as suggested by Riedo *et al.*[8] The second frequency is a sliding frequency, V/a, where a is the lattice constant of the surface. At this frequency, the tip atom follows synchronous motion with the support point and the slip is brought forward inducing reduction of the average friction force.

Our aim is to clarify both the atomistic mechanism and the condition of the dynamic superlubricity of nanometer-sized contacts observed by Socoliuc *et al.*[9] We used the Tomlinson model at a finite temperature and used Ermak's

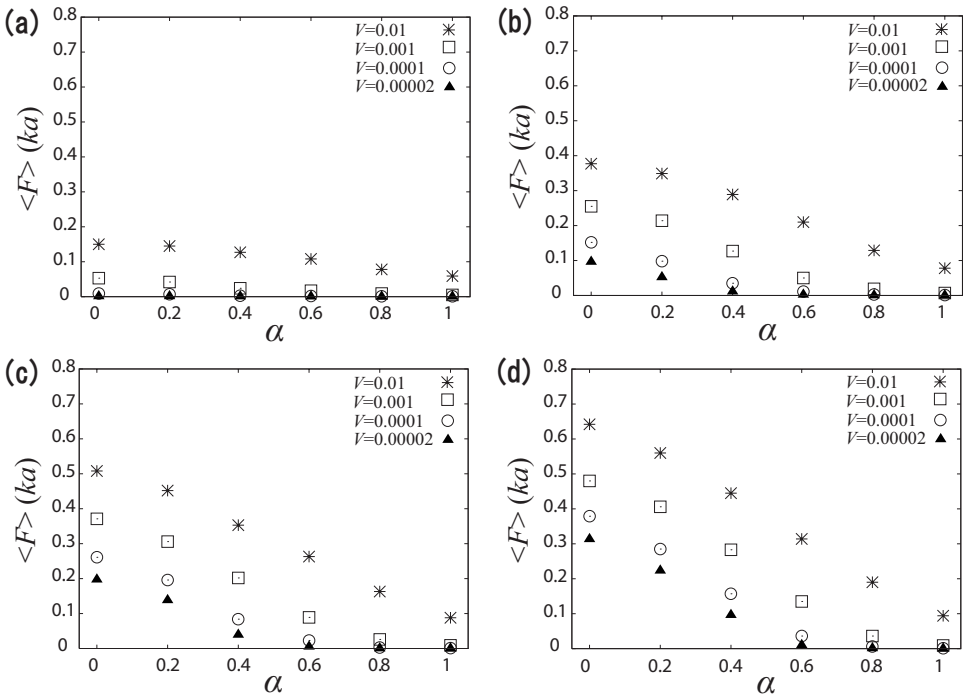

FIG. 1. The relation between the time-averaged friction force $\langle F\rangle$ and the oscillation amplitude α of ac modulation at four sliding velocities V, for $\eta=3$ (a), 5 (b), 6 (c), and 7 (d). Here, $\xi=2$, $T=0.016$, $f=0.05$ are assumed.

algorithm[21] to solve the Langevin equation numerically. We address the dependence of the friction on the corrugation amplitude of the surface potential, a damping coefficient, sliding velocity, and temperature.

II. FORMULATION

The total interaction energy in the one-dimensional Tomlinson model is given as

$$E(x,R) = -U\cos\left(\frac{2\pi x}{a}\right) + \frac{k}{2}(R-x)^2, \tag{1}$$

where x is the coordinate of the tip atom and R is the position of the support point of FFM. The first term of Eq. (1) is periodic potential of the substrate with the lattice constant, a, and the second term is the elastic interaction with an elastic constant, k, between the tip atom and the support point. We represent the effect of the normal modulation on the lateral tip motion by assuming that the corrugation amplitude of the surface potential changes with time as,[9]

$$U(t) = U_0(1 + \alpha\cos 2\pi f t). \tag{2}$$

When $\alpha=0$ without ac modulation, the stick-slip motion occurs in the following condition.[5,15]

$$\eta \equiv \frac{4\pi^2 U_0}{ka^2} > 1. \tag{3}$$

When the support point R is scanned at the velocity V, the dynamics of the tip atom is described by the Langevin equation,[7]

$$m\ddot{x} + m\xi\dot{x} = -\frac{\partial E(x,Vt)}{\partial x} + f_r, \tag{4}$$

where R is set as $R=Vt$. Here, m is the mass of the tip, ξ is the damping coefficient representing the energy dissipation. f_r is a random force that is related to the damping coefficient ξ by the fluctuation dissipation theorem.

$$\langle f_r(t) f_r(t')\rangle = 2m\xi k_B T\delta(t-t'), \tag{5}$$

where k_B is the Boltzmann constant and T is the absolute temperature. We used Ermak's algorithm[21] to solve the Langevin equation numerically. The friction force $F(R)$ of FFM is given by,

$$F = k(R-x). \tag{6}$$

Hereafter, we take a as the unit of length and ka^2 as the unit of energy. Further, we take m as unity, *i.e.* the unit of time is $\sqrt{m/k}$. In this unit system of $a=1$, $ka^2=1$, and $m=1$, our system is characterized by four dimensionless parameters: the damping coefficient $\xi\sqrt{m/k}$, the surface potential amplitude U_0/ka^2, sliding velocity $V\sqrt{m/ka^2}$, and the temperature k_BT/ka^2. We used mainly following values assumed by Socoliuc *et al.*;[9] $a=0.5$ nm, $k=1$ N/m, $f_{nt}=178$ kHz, $f=56.7$ kHz, and $V=10$ nm/s. Here, f_{nt} is the resonant frequency of a nanotip, $f_{nt}=\frac{1}{2\pi}\sqrt{\frac{k}{m}}$. These have dimensionless values of $f_{nt}=0.16$, $f=0.051$, $V=1.8\times10^{-5}$. The unit of force, ka, becomes 0.5 nN and the unit of energy, ka^2, does 1.56 eV. In this unit, a room temperature is $T=0.016$. The critical value of the damping coefficient is given by, $\xi_{cr}=4\pi f_{nt}$, and its dimensionless value is 2. In the latter part of this paper, we denote these dimensionless parameters simply as ξ, U_0, T, V and f.

III. NUMERICAL RESULTS

At first, we present in Fig. 1 the time-averaged friction force $\langle F\rangle$ at a room temperature ($T=0.016$) for the surface

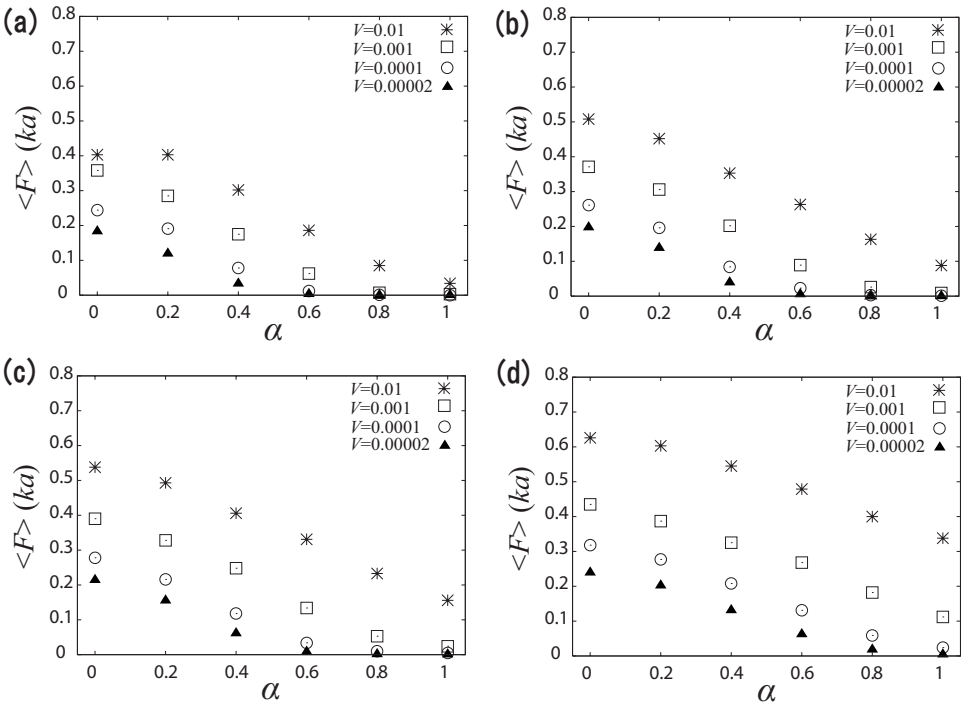

FIG. 2. The relation between the time-averaged friction force $\langle F\rangle$ and the oscillation amplitude α of ac modulation at four sliding velocities V, for $\xi=0.4$ (a), 2 (b), 4 (c), and 10 (d). Here, $\eta=6$, $T=0.016$, $f=0.05$ are assumed.

potential amplitude, $\eta=3,5,6,7$, as a function of relative ac modulation amplitude, α. Here, we assumed $\xi=2$, *i.e.* the critical damping coefficient. It can be seen in Fig. 1 that $\langle F\rangle$ decreases monotonically with increasing α and it vanishes above the critical value α_{cr}. The value of α_{cr} depends on both the surface potential corrugation, η, and the sliding velocity, V. If the critical value is determined by Eq. (3) with use of the minimum corrugation amplitude, $U_0(1-\alpha)$, with ac modulation, as pointed out by Socoliuc *et al.*,[9] α_{cr} can be predicted as,

$$\alpha_{cr}^0 = 1 - \eta^{-1}. \tag{7}$$

The calculated α_{cr} at a room temperature for $V=0.000\,02$ is much smaller than this predicted value, because of thermally activated hopping of the tip. As for the scanning velocity dependence, $\langle F\rangle$ decreases monotonically with decreasing velocity since the thermally activated hopping is enhanced by lowering the velocity. In the experiment on NaCl surface by Socoliuc *et al.*,[9] $\langle F\rangle=0.11$ nN was observed at the scanning velocity of $V=10$ nm/s without ac modulation. This

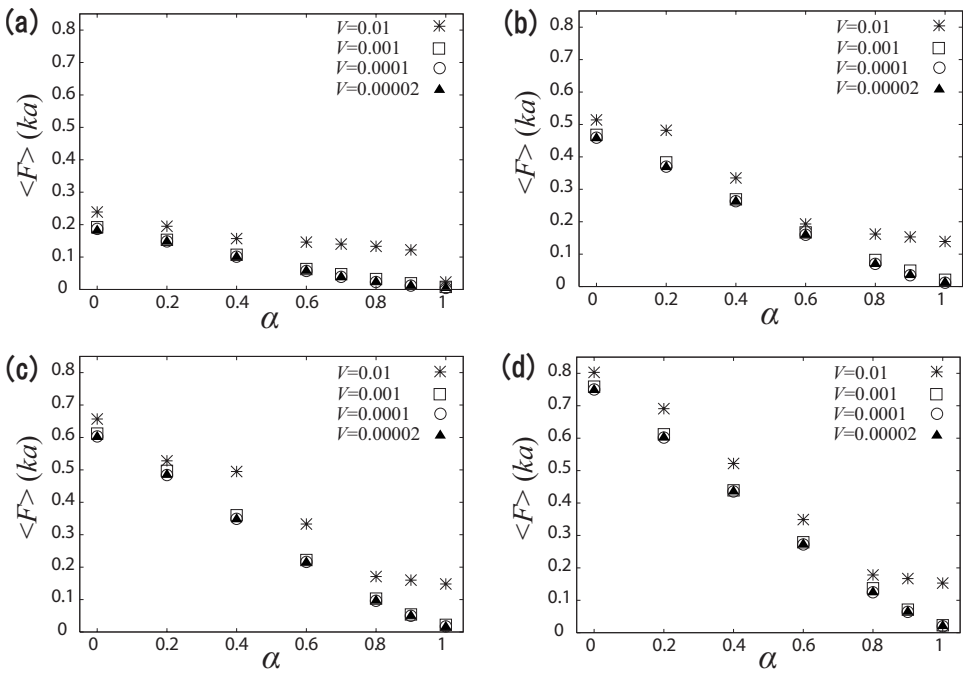

FIG. 3. The relation between the time-averaged friction force $\langle F\rangle$ and the oscillation amplitude α of ac modulation at four sliding velocities V, for $\eta=3$ (a), 5 (b), 6 (c), and 7 (d). Here, $\xi=2$, $T=0$, and $f=0.05$ are assumed.

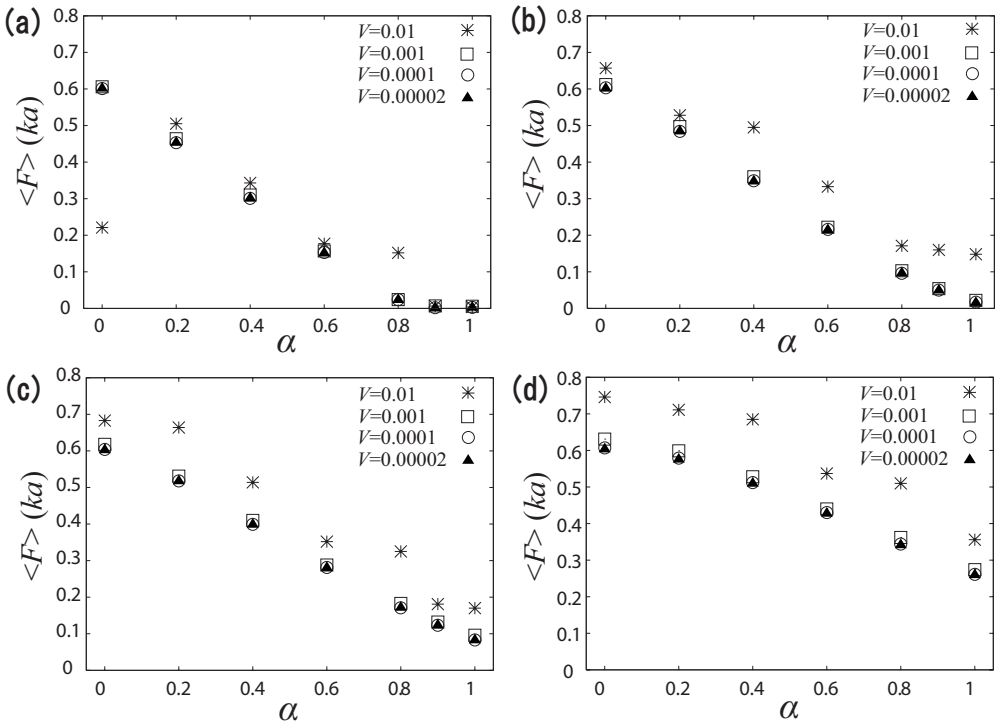

FIG. 4. The relation between the time-averaged friction force $\langle F\rangle$ and the oscillation amplitude α of ac modulation at four sliding velocities V, for $\xi=0.4$ (a), 2 (b), 4 (c), and 10 (d). Here, $\eta=6$, $T=0$, and $f=0.05$ are assumed.

friction force is approximately obtained at $\eta=6$ in our simulation at the scan velocity of $V=0.000\,02$. This corresponds to the corrugation amplitude of the surface potential of $U_0=0.24$ eV.

Second, we present in Fig. 2 the dependence of the time-averaged friction force at a room temperature on the damping coefficient, ξ, in the case of $\eta=6$. It is seen that both $\langle F\rangle$ and α_{cr} increase slightly as ξ increases. It should be mentioned that the superlubricity can be observed at $V=0.00002$ in the extremely overdamped situation of $\xi=10$.

To clarify the finite temperature effects in Figs. 1 and 2, we present in Figs. 3 and 4 the corresponding dependences of the time-averaged friction force $\langle F\rangle$ at zero temperature. The observed remarkable velocity dependence of $\langle F\rangle$ at a room temperature vanishes almost completely at $T=0$ in low-velocity region below $V\leq 0.001$ and $\langle F\rangle$ becomes much larger than that at a room temperature, by suppression of thermally activated hopping. In Fig. 3 where the critical damping coefficient is assumed, the calculated α_{cr} is a little larger than the predicted value of Eq. (7). In the underdamped case at $\eta=6$ in Fig. 4(a), α_{cr} approaches the predicted value, $\alpha_{cr}^0=0.83$ in low velocities. Socoliuc *et al.* determined the surface potential amplitude as $\eta=3$ from the observed value of $\langle F\rangle=0.11$ nN without ac modulation.[9] This suggests that their calculation was performed at $T=0$. In high velocities, on the other hand, $\langle F\rangle$ depends on the sliding velocity: $\langle F\rangle$ at $V=0.01$ is larger than those at lower velocities, except the case of $\alpha=0$ and $\xi=0.4$ in Fig. 4(a). In this case, double slips appear as shown in Fig. 6(a) and, hence, the average friction force can be reduced remarkably.[15] With ac modulation, the average friction force increases with ξ and the superlubricity is suppressed for the overdamped case of $\xi>\xi_c$ in Fig. 4.

Now, we investigate how the dynamic superlubricity appears and how the damping coefficient, the sliding velocity and temperature affect the dynamic superlubricity. In Fig. 5, we plot the relation between the tip coordinate x and the support point R at $T=0$ in the underdamped case of $\xi=0.4$ and the overdamped case of $\xi=4$. Here, $\eta=6$, $f=0.05$, and $V=0.001$ are assumed. In the case of $\alpha=0$, the stick-slip motion occurs and the slip position does not depend on ξ. This means that the average friction force is almost independent of the damping coefficient at $T=0$ in low-sliding velocities. In the case of $\alpha=0.6$ with ac modulation, the oscillation with a frequency f is superimposed at the stick point and the position of abrupt slip precedes that for $\alpha=0$ and hence the average friction force is reduced. In the case of $\alpha=0.9$, x changes continuously through $x=1.5(2.5)$ at $R=1.5(2.5)$ without an abrupt slip for $\xi=0.4$, as seen in Fig. 5(a) and the dynamic superlubricity is actuated. On the other hand, for $\xi=4$, the stick-slip motion survives at $\alpha=0.9$ with an abrupt slip and the superlubricity does not occur. In this overdamped case, the growth rate of the oscillation amplitude of the tip atom at the stick point is suppressed and the smooth movement of a tip via the turning point, $x=1.5(2.5)$ at $R=1.5(2.5)$, is interrupted. As for the damping coefficient dependence of $\langle F\rangle$ with ac modulation, $\langle F\rangle$ increases with ξ, caused by delay of the slip point. In Fig. 6, we plot the relation between the tip coordinate x and the support point R in the case of high velocity of $V=0.01$ at $T=0$ for $\xi=0.4$ and 4, $\eta=6$, $f=0.05$. In the case of $\xi=0.4$, a double slip is induced at $\alpha=0$ in Fig. 6(a) and the average friction force is reduced in comparison with that at a lower sliding velocity of $V=0.001$. The double slips occur if the tip atom can arrive at the next nearest local minimum of the total interaction energy, overcoming the middle energy barrier.[15] Hence, the low-damping coefficient assists in the appearance of double slips because the energy dissipation is suppressed. The fast scanning velocity also assists in the appearance of double slips, since the rapid time variation in $E(x,Vt)$ lowers the

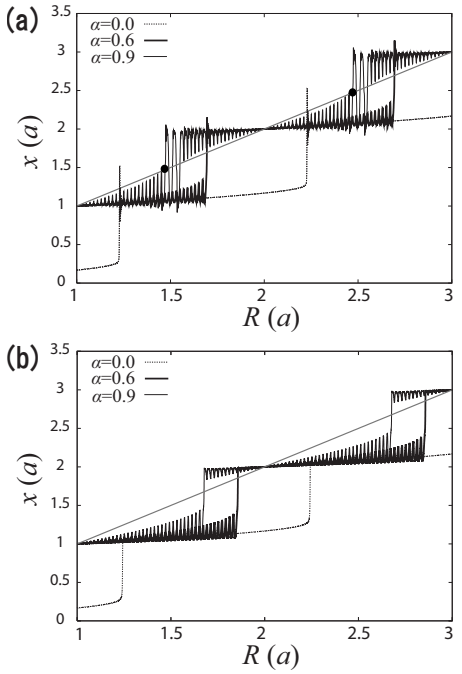

FIG. 5. The relation between the tip coordinate x and the support point R in the dynamical simulation at $T=0$, for $\xi=0.4$ (a) and 4 (b). Here, $\eta=6$, $f=0.05$, and $V=0.001$ are assumed. The turning point and the relation of $x=R$ are also plotted.

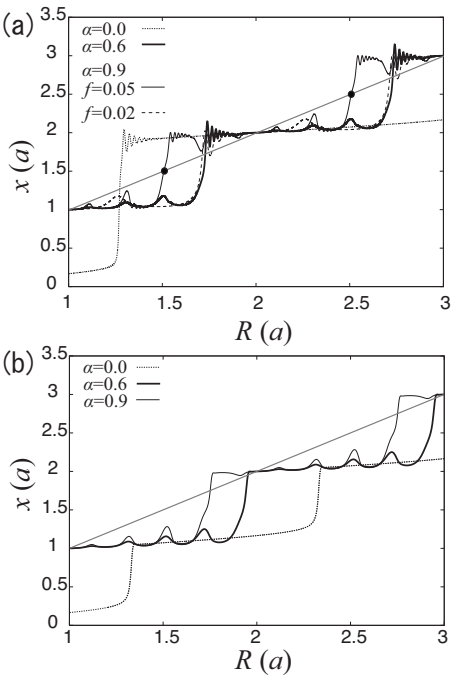

FIG. 6. The relation between the tip coordinate x and the support point R in the dynamical simulation at $T=0$, for $\xi=0.4$ (a) and 4 (b). Here, $\eta=6$, $f=0.05$, and $V=0.01$ are assumed. In (a), the result of $f=0.02$ is also plotted at $\alpha=0.9$ by a dashed line. The turning point and the relation of $x=R$ are also plotted.

barrier height and induces instability of the nearest local minimum. On the other hand, with ac modulation, a single slip is induced at $\alpha=0.6$ while a continuous change in a tip atom position through the turning point, $x=1.5(2.5)$ at $R=1.5(2.5)$, can be seen at $\alpha=0.9$. For $\xi=4$ in Fig. 6(b), the stick-slip motion survives still at $\alpha=0.9$ and the superlubricity does not appear. The slip points in Fig. 6(b) are delayed than those in Fig. 5(b) at $V=0.001$ and hence $\langle F\rangle$ in the case of $\xi=4$ is increased for high-scan velocity.

Here, we consider the modulation frequency dependence of $\langle F\rangle$ at $T=0$. If f is changed to 0.02 at $\alpha=0.9$ for $V=0.001$ in Fig. 5(a), the slip points shift only slightly ahead from the turning points and the calculated result almost overlaps with one at $f=0.05$. It results in slight increase in the average friction force to $\langle F\rangle=0.018$ from the vanishing value at $f=0.05$. This suggests that $\langle F\rangle$ can approach to zero with decreasing sliding velocities independent on the individual value of the modulation frequency, i.e., the dynamic superlubricity can be allowed at $T=0$ if the condition of $f \gg V/a$ is satisfied in the underdamped case. In Fig. 6(a) for $V=0.01$, on the other hand, the above condition is not well satisfied at both $f=0.05$ and $f=0.02$. However, the dynamic superlubricity occurs at $\alpha=0.9$ for $f=0.05$, but the stick-slip motion is revived for $f=0.02$, as shown in Fig. 6(a) by the broken line. It results in a large increase in $\langle F\rangle=0.17$ at $f=0.02$ and the observed superlubricity at $f=0.05$ disappears. This indicates that the observed superlubricity at $T=0$ for high-sliding velocity is induced by the synchronous motion of the tip with the support point such as the oscillating tip just passes the turning point. The synchronous motion is allowed at $f=0.05$ but not at $f=0.02$. Hence, the superlubricity observed at $f=0.05$ for $V=0.01$ disappears at $f=0.02$. Even if the synchronous motion is not allowed, however, it is possible to pass the vicinity of the turning point in the underdamped case if the condition of $f \gg V/a$ is satisfied.

In Fig. 7, we plot the relation between the tip coordinate x and the support point R at a room temperature for $\xi=0.4$ and 4, $\eta=6$, $f=0.05$, and $V=0.0001$. In the case of $\alpha=0$, stick-slip motion occurs with a single slip while a thermal fluctuation is superimposed at the stick point. The slip position is a little earlier for $\xi=0.4$ than that for $\xi=4$ on average, without ac modulation. This causes a little smaller time averaged friction force without ac modulation by decreasing the damping coefficient. Furthermore, it can be seen that the slip position is much earlier than that at $T=0$ (Fig. 5), induced by thermally activated hopping. It should be noticed that the results at $T=0$ are almost independent on V for $V \leq 0.001$ in Figs. 3 and 4. Similarly, the relation between the tip coordinate x and the support point R does not depend on V at $T=0$ for $V \leq 0.001$. In the case of $\alpha=0.6$ with ac modulation, on the other hand, the slip point of a tip is brought forward remarkably for both $\xi=0.4$ [Fig. 7(b)] and 4 [Fig. 7(d)], and the average friction force is reduced dramatically [see Figs. 2(b) and 2(c)]. The dynamic superlubricity can be actuated at a room temperature for $\xi=0.4$ at a much reduced ac modulation amplitude of $\alpha=0.6$ than the predicted value of $\alpha_{cr}^{0}=0.83$ determined from the minimum corrugation amplitude, $U_0(1-\alpha)$, with ac modulation. For the static surface potential with the corrugation amplitude of $U_0(1-\alpha)$, on the other hand, the average friction force $\langle F\rangle$ diminishes at a room temperature at $V=0.0001$ for both damping coefficients, $\xi=0.4$ and 4. This suggests that the dynamical superlubricity at a room temperature is also determined by the minimum

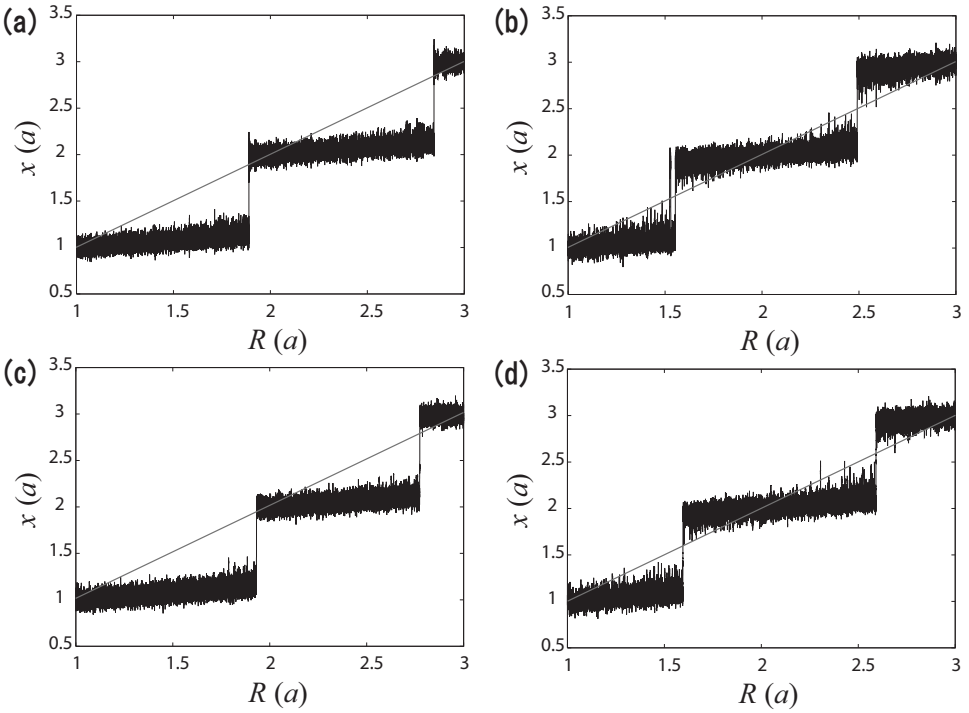

FIG. 7. The relation between the tip coordinate x and the support point R in the dynamical simulation at $T=0.016$, for (a) $\xi=0.4$ and $\alpha=0$, (b) $\xi=0.4$ and $\alpha=0.6$, (c) $\xi=4$ and $\alpha=0$, (d) $\xi=4$ and $\alpha=0.6$. Here, $\eta=6$, $f=0.05$, and $V=0.0001$ are assumed. The relation of $x=R$ is also plotted.

corrugation amplitude with ac modulation. The enough time for the thermally activated hopping at the minimum corrugation amplitude can be assured if the condition of $f \gg V/a$ is sufficiently satisfied.

Finally in Fig. 8, we show a part of Figs. 7(a) and 7(c) in the enlarged scale of R. The thermal excitation of oscillation of the tip can be seen clearly at the stick point without ac modulation. The oscillation amplitude is larger for $\xi=0.4$ than for $\xi=4$, while the thermal noise is much stronger for $\xi=4$ than for $\xi=0.4$. Hence, the resultant thermal fluctuation of the tip position has a similar magnitude at a room temperature insensitive to the value of the damping coefficient, contrary to the forced oscillation at $T=0$ of the tip by ac modulation of the corrugation amplitude.

IV. DISCUSSION AND CONCLUSION

We consider why the tip takes such a motion as shown in Figs. 5–7. In the adiabatic approximation, the coordinate x of the tip is assumed to take the local minimum of the total interaction energy, $E(x,R)$, for a given support position R. The local minimum of $E(x,R)$ is given by the relation,

$$R = x + \frac{2\pi U}{ka}\sin\left(\frac{2\pi x}{a}\right). \tag{8}$$

In the case of $\eta<1$, the tip coordinate x is a monotonic increasing continuous function of R and the stick-slip motion of the tip atom does not occur. On the other hand, in the case of $\eta>1$, x becomes a multivalued function of R and a discontinuous jump of x is induced at $R=R_c$. Here, R_c is the extreme value of $R(x)$ and is given by,

$$R_c = \frac{a}{2\pi}\left\{\arccos\left[\frac{-ka^2}{(2\pi)^2 U}\right] + \frac{(2\pi)^2 U}{ka^2}\sqrt{1-\left[\frac{ka^2}{(2\pi)^2 U}\right]^2}\right\}. \tag{9}$$

We plot the relation of Eq. (8) in Fig. 9, where U is assumed to be $U_0(1\pm\alpha)$ at $\eta=6$. If the sliding velocity V is sufficiently low, the tip position x oscillates between $x_+(R)$ and $x_-(R)$, where $x_\pm(R)$ is obtained from Eq. (8) with U

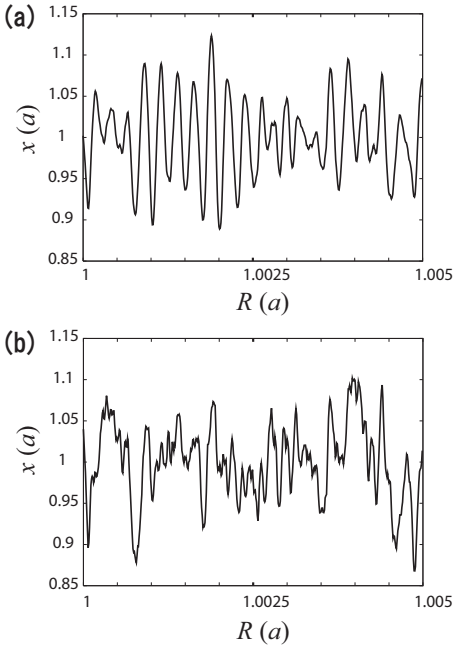

FIG. 8. The relation between the tip coordinate x and the support point R in a range of $1a \le R \le 1.005a$, for (a) $\xi=0.4$ and (b) $\xi=4$. Here, $T=0.016$, $\alpha=0$, $\eta=6$, and $V=0.0001$ are assumed.

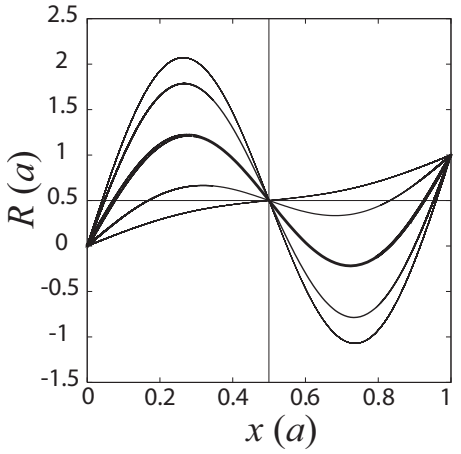

FIG. 9. The relation of Eq. (8) between the position of the support point R and the tip coordinate x, for $U=U_0(1\pm\alpha)$. Here, $\eta=6$, $\alpha=0$ (thick solid line), $\alpha=0.6$ (medium solid line), and $\alpha=0.9$ (thin solid line) are assumed.

$=U_0(1\pm\alpha)$. In the case of $\alpha<\alpha_{cr}^0$, $x_-(R)$ becomes a multivalued function of R as the case of $\alpha=0.6$ in Fig. 9 and the slip occurs at $R=R_c=0.67$ at the minimum corrugation amplitude with ac modulation, $U_0(1-\alpha)$. However, for $\alpha>\alpha_{cr}^0$, $x_-(R)$ becomes a single-valued function of R as the case of $\alpha=0.9$ in Fig. 9 and the tip is allowed to pass the turning point of $x=R=(n+0.5)a$ with an integer n. We call this point as the turning point, since the tip can change continuously the stick position through the turning point, i.e., the top position of the surface potential without elastic deformation of the tip. In the adiabatic approximation, the stick-slip motion can be suppressed for $\alpha\geq\alpha_{cr}^0$, as predicted by Socoliuc *et al.*[9] In the dynamical case, however, the oscillation amplitude of the tip at the stick point depends also on the damping coefficient ξ and the range of motion of the tip coordinate x is limited within a smaller range, as seen in Fig. 5(b). Hence, the tip atom cannot pass through the turning point even for $\alpha>\alpha_{cr}^0$ with increasing ξ. Hence, the dynamic superlubricity does not occur for overdamped case at $T=0$. However, the dynamic superlubricity can be actuated easily at a room temperature even for $\alpha<\alpha_{cr}^0$ in both the underdamped and the overdamped cases, by assistance of thermally activated hopping. Indeed, the slip position at a room temperature is remarkably brought forward than those at $T=0$, $R=R_c+na$ with an integer n, as seen in Figs. 7(b) and 7(d).

With respect to the condition for appearance of the dynamic superlubricity, Socoliuc *et al.* pointed out following two conditions.[9]

$$f_{nt}\gg f\gg V/a,$$

$$f\xi\ll 4\pi f_{nt}^2. \tag{10}$$

The relation of $f_{nt}\gg f$ in the first condition in Eq. (10) is necessary for the tip to follow the oscillation with a frequency of f. The second condition in Eq. (10) means that the effect of the damping term is much weaker than one of the spring term in the equation of motion of Eq. (4). From this second condition, the relation of $\xi\ll 6.4$ is derived for $f=0.05$ and $f_{nt}=0.16$. Indeed, this condition is satisfied for the underdamped case of $\xi=0.4$ and superlubricity is observed at $T=0$ in Fig. 4(a). On the other hand, the superlubricity can be observed at a room temperature also for the overdamped cases of $\xi=4$ and 10, as seen in Fig. 2. This indicates that the second condition of Eq. (10) can be relaxed largely at a room temperature. The elimination of the condition, $f\xi\ll 4\pi f_{nt}^2$, means that achieving superlubricity in a dynamic way becomes very efficient at a room temperature. However, the condition of $f_{nt}\gg f\gg V/a$ must be satisfied to assure the thermally activated hopping in the vicinity of the minimum corrugation amplitude with ac modulation.

In summary, we studied the mechanism of dynamic superlubricity of the atomic contact of a friction force microscope, using the dynamical simulation of the Tomlinson model at a room temperature. The effect on the dynamic superlubricity of the corrugation amplitude of surface potential, sliding velocity, a damping coefficient, and temperature are clarified. The dynamic superlubricity at zero temperature is induced above the critical amplitude of ac modulation by transit of the tip via the "turning point," and it is realized for the underdamped case if the sliding velocity, V, is much lower than the ac modulation frequency, f, i.e., $f\gg V/a$. The dynamic superlubricity at a room temperature, on the other hand, can be actuated efficiently at a much smaller critical amplitude than that at $T=0$, assisted by thermally activated hopping. It can be realized also for the overdamped case, if the condition of $f\gg V/a$ is sufficiently satisfied.

ACKNOWLEDGMENTS

This work was supported by a Grant No. 18540313 in Aid for Scientific Research from Ministry of Education, Culture, Sports, Science, and Technology.

*junj@ee.uec.ac.jp; http://andes.ee.uec.ac.jp/~junj/
†natori@ee.uec.ac.jp

[1] C. M. Mate, G. M. McClelland, R. Erlandsson, and S. Chiang, Phys. Rev. Lett. **59**, 1942 (1987).
[2] M. Hirano and K. Shinjo, Phys. Rev. B **41**, 11837 (1990).
[3] M. Dienwiebel, G. S. Verhoeven, N. Pradeep, J. W. M. Frenken, J. A. Heimberg, and H. W. Zandbergen, Phys. Rev. Lett. **92**, 126101 (2004).
[4] M. Igarashi, A. Natori, and J. Nakamura, Phys. Rev. B **78**, 165427 (2008).
[5] A. Socoliuc, R. Bennewitz, E. Gnecco, and E. Meyer, Phys. Rev. Lett. **92**, 134301 (2004).
[6] S. Y. Krylov, K. B. Jinesh, H. Valk, M. Dienwiebel, and J. W. M. Frenken, Phys. Rev. E **71**, 065101(R) (2005).
[7] Y. Sang, M. Dube, and M. Grant, Phys. Rev. Lett. **87**, 174301 (2001).

[8] E. Riedo, E. Gnecco, R. Bennewitz, E. Meyer, and H. Brune, Phys. Rev. Lett. **91**, 084502 (2003).
[9] A. Socoliuc, E. Gnecco, S. Maier, O. Pfeiffer, A. Baratoff, R. Bennewitz, and E. Meyer, Science **313**, 207 (2006).
[10] E. Gnecco, Nature (London) **461**, 178 (2009).
[11] G. A. Tomlinson, Philos. Mag. **7**, 905 (1929).
[12] Y. Hoshi, T. Kawagishi, and H. Kawakatsu, Jpn. J. Appl. Phys., Part 1 **39**, 3804 (2000).
[13] K. L. Johnson and J. Woodhouse, Tribol. Lett. **5**, 155 (1998).
[14] C. Fusco and A. Fasolino, Phys. Rev. B **71**, 045413 (2005).
[15] J. Nakamura, S. Wakunami, and A. Natori, Phys. Rev. B **72**, 235415 (2005).
[16] S. N. Medyanik, W. K. Liu, I. H. Sung, and R. W. Carpick, Phys. Rev. Lett. **97**, 136106 (2006).
[17] E. Gnecco, R. Bennewitz, T. Gyalog, C. Loppacher, M. Bammerlin, E. Meyer, and H.-J. Güntherodt, Phys. Rev. Lett. **84**, 1172 (2000).
[18] A. Schirmeisen, L. Jansen, H. Holscher, and H. Fuchs, Appl. Phys. Lett. **88**, 123108 (2006).
[19] Z. Tshiprut, S. Zelner, and M. Urbakh, Phys. Rev. Lett. **102**, 136102 (2009).
[20] M. Igarashi, J. Nakamura, and A. Natori, Jpn. J. Appl. Phys. **46**, 5591 (2007).
[21] M. P. Allen and D. J. Tildesley, *Computer Simulations of Liquids* (Clarendon, Oxford, 1990).